AIP | Applied Physics Letters

Electrical passivation of nonselective bio molecules in carbon nanotubes: Effect of pulse train in serum

Seok Hyang Kim, Jun-Myung Woo, Seongwook Choi, and Young June Park

Citation: Applied Physics Letters **106**, 263701 (2015); doi: 10.1063/1.4923241
View online: http://dx.doi.org/10.1063/1.4923241
View Table of Contents: http://scitation.aip.org/content/aip/journal/apl/106/26?ver=pdfcov
Published by the AIP Publishing

Electrical passivation of nonselective bio molecules in carbon nanotubes: Effect of pulse train in serum

Seok Hyang Kim,[1] Jun-Myung Woo,[2] Seongwook Choi,[1] and Young June Park[1,a)]
[1]*Department of Electrical and Computer Engineering, Seoul National University, Seoul 151-744, South Korea*
[2]*DRAM Design Team, Memory business, Samsung Electronics Co., Ltd., Giheung 466-711, South Korea*

(Received 26 February 2015; accepted 16 June 2015; published online 29 June 2015)

We present an experimental and simulation study about a desorption of albumin, a representative nonselective molecules in serum, on carbon nanotube (CNT) surface as an electrical bio sensing channel under the pulse train condition. The motivation of the study on binding kinetics between CNT surface and albumin is to suppress the adsorption of nonselective proteins in blood such as albumin, thereby enhancing the selectivity of the electrical biosensor. To theoretically model the behavior of molecules and ions under the step pulse bias, the physics on the reaction rate, mass transport, and the resulting surface pH-value are considered using the Poisson and drift-diffusion equations. For the simulation model, the phosphate buffered saline is considered as the electrolyte solution and albumin is considered as a representative charged molecule for nonspecific binding in serum. Both the transient simulation and experimental result indicate that the suppression of the nonspecific binding under the pulse train is due to the unsymmetrical field force experienced by the protein during the pulse transitions (high to low and low to high) and the non-symmetry is caused by the different transient times between the electric field and the charge/discharge of the protein according to the surface pH modulation in serum. The experimental and simulation results clearly indicate that the pulse bias suppresses the nonselective bio molecules adsorption at the CNT surface so that the selectivity of the electrical biosensor for detecting the target molecules can be enhanced. © *2015 AIP Publishing LLC*. [http://dx.doi.org/10.1063/1.4923241]

Electrical biosensors have many advantages over non-electrical sensor devices based on other principles such as a surface plasmon resonance (SPR), mechanics and so on.[1–3] The electrical nano-biosensors, in particular, have additional advantages in a sensing speed, a detection accuracy, and a capability of integration on the semiconductor devices.[4,5] However, for the affinity-based electrical biosensor, a selectivity is critical issues limiting the biosensor performance.[6] The selectivity issue is related with probe-target binding efficiency and nonspecific binding, in which noisy bio molecules stick to the probe layer, preventing target binding or causing a false positive signal. Sometimes, washing the sensor before readout is introduced to reduce the nonspecific binding by removing the unwanted adsorbed molecules while leaving the probe-target binding. But, in the real-time measurement for the Point-of-Care (PoC) application, this washing step should be avoided.[7,8] Hence, developing the pure electrical way is a crucial activity for PoC applications by modulating the nonspecific binding of bio molecules in serum.

Theoretically, one of the key physical terms which governs the adsorption is an electrostatic interaction forces between the charged surface (the adsorption site) and bio molecule because bio molecules are also charged depending on the solution pH and isoelectric point (pI) of bio molecules.[9,10] With the background, we propose a modulation of adsorption ratio based on "pulse train" to change the electrostatic environment at the surface. Under the application of pulse trains across the electrodes (in our case, the source and drain), the H^+ distribution near surface can be controlled in even buffer solutions. In this way, the nonspecific molecules in serum could be electrically passivated, and thus, it is possible to remove the additional washing steps and further treatments of carbon nanotube (CNT) surface[11,12] (e.g., Tween-20, polyethylene glycol [PEG], or the like).

The purpose of this paper is to give an understanding and controlling of the physical phenomena taking place in the solid-physiological solution interface under the electrical pulse train. The effects of the pulse bias voltage on the nonselective binding events between the CNT and proteins in serum can only be understood by combined efforts of the theoretical simulation and experiments. To theoretically model the behavior of molecules and ions under the pulse train, the physics about reaction rate, mass transport, and the resulting surface pH-value are considered to solving the Poisson and drift-diffusion equations. In addition, we report the electrical and optical observations for nonspecific binding of biomolecules in serum under the electrical pulse train using the biosensor platform developed in our group.[13]

For the physical model of the binding event at the electrode-electrolyte surface, the transport of molecules and ions in the electrolyte and their kinetics are coupled with the Poisson equation as follows in 1-dimensional space.

In the electrolyte solutions, the movement of ion carriers is governed by the drift and diffusion similar to the transport of the electrons and holes in the semiconductor. Accordingly, the continuity equation of ion and the flux are represented by

a)Author to whom correspondence should be addressed. Electronic mail: ypark@snu.ac.kr

$$\frac{\partial[n^{\pm}]}{\partial t} = -\nabla \cdot \boldsymbol{F}_{n^{\pm}} = -\nabla \cdot \left\{ \pm \mu_{n^{\pm}}[n^{\pm}]\nabla\psi - D_{n^{\pm}}\nabla[n^{\pm}] \right\}, \tag{1}$$

where $\mu_{n\pm}$ and $D_{n\pm}$ are the mobility and the diffusion coefficient of the charged particles considered in this work.

The electrical potential and charged carriers in the electrolyte solution are governed by the Poisson equation as

$$\nabla \cdot \varepsilon(-\nabla\psi) = q([n^{+}] - [n^{-}]), \tag{2}$$

where ε is the permittivity of electrolyte solution, ψ is the electrical potential, and $[n^{+}]$ and $[n^{-}]$ are the concentration of the charged particles considered in this work including cations (Na^{+}, K^{+}, H^{+}) and anions (Cl^{-}, OH^{-}, HPO_4^{2-}, $H_2PO_4^{-}$) in the electrolyte solution and charged proteins (Albumin). The simulation parameters such as mobility and reaction constants are obtained from references.[14–20]

The electrical potential ψ_0 is applied to the electrode as a Dirichlet boundary condition with respect to bulk solution which is grounded by the reference electrode. For the simulation, above electrostatic and transport equations are solved self-consistently using in-house simulation codes[13,21,22] including the chemical reactions of the following cases: (1) no buffer reaction, (2) a phosphate buffered saline (PBS) solution, and (3) a PBS solution with albumin.

In a solution without addition of a buffer, only the species H^{+}, OH^{-}, Na^{+} (0.1 M), and Cl^{-} (0.1 M) contribute to the current transport. Figure 1 shows the theoretical ion distribution (H^{+}) *versus* distance after applying step pulse voltage (0.5 V, −0.5 V) for unbuffered solutions. In the case of a positive bias (Figure 1(a)), the positively charged ions (H^{+}, Na^{+}) are swept away and the negatively charged ions (OH^{-}, Cl^{-}) congregated at the near surface region (within 0–4 nm) by a high external electric field due to the extended electric double layer on transient state after pulse bias. The other way, in the case of a negative bias (Figure 1(b)), the negatively charged ions are swept away and the positively charged ions congregated. Since unbuffered solutions are unable to compensate the generation/recombination of H^{+} like in the buffer solution, the surface pH can be altered quite easily by applying bias.

For the PBS solution, the interaction between buffer and water are included in the model which can be written as

$$H_3PO_4 \underset{K_{a1}}{\leftrightarrow} H_2PO_4^{-} + H^{+} \underset{K_{a2}}{\leftrightarrow} HPO_4^{2-} + 2H^{+} \underset{K_{a3}}{\leftrightarrow} PO_4^{3-} + 3H^{+}, \tag{3}$$

where $H_mPO_4^{n-}$ (n: 0,1,2,3, m: 0,1,2,3) is the phosphate ion and $K_{a1,2,3}$ (K_{a1}: 7.25×10^{-3} M^{-1}, K_{a2}: 6.31×10^{-8} M^{-1}, K_{a3}: 4.80×10^{-13} M^{-1}) is the association constant between phosphate ion and H^{+}.

The local concentrations of H^{+} in the diffuse layer of a buffer solution are shown in Figures 2(a) and 2(b) for the positive and negative bias, respectively. It was explained in the above paragraph that, by applying positive or negative bias to the unbuffered solution, the surface pH is changed to acid or alkaline. But, in a buffer solution, the surface pH shows a different result under positive or negative bias. In case of positive bias, the concentration of H^{+} near the surface is almost the same as the bulk concentration. This is due to the influence of the buffering reaction with H^{+} via the reaction shown in Eq. (3), so that the buffer maintains a constant value for the local pH. However, in case of negative bias, the local ion distribution for the buffered solution follows the same tendency of that for the unbuffered case. Since the buffer ion concentration on the electrode surface is depleted by the applied bias, the buffer reaction cannot keep the concentration of surface H^{+} the same as that in bulk case. As a result, the buffer action is lost near the surface under negative bias (showing the steep gradient in Figure 2(b)). In summary, in the buffer solution, the surface pH can deviate from the bulk pH when pulse bias is applied.

For the simulation of the buffer solution with a nonspecific protein, the protein (albumin) is assumed to be globular[23,24] with point charges at the center and is embedded in an environment with a high permittivity ε_w ($78 \times \varepsilon_0$) representing the solvent.

The charging state of albumin is determined with the reaction as

$$H_2 - Albumin^{n-} \underset{K_{a4}}{\Longleftrightarrow} H - Albumin^{(n+1)-} + H^{+} \underset{K_{a5}}{\Longleftrightarrow} Albumin^{(n+2)-} + 2H^{+}, \tag{4}$$

where K_{a4} ($7.94 \times 10^{5}\,M^{-1}$) and K_{a5} ($1.26 \times 10^{9}\,M^{-1}$) is the association constant[19] between albumin and H^{+}. Hence, the charging state of albumin is determined by the concentration of H^{+} near the albumin.

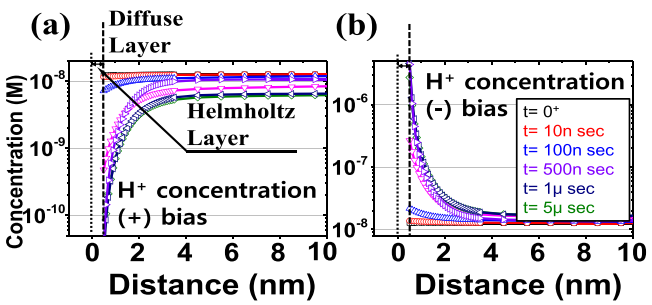

FIG. 1. Simulation results on H^{+} distribution *vs.* distance from surface after unit pulse is applied in unbuffered solution (H^{+}, OH^{-}, Na^{+}, Cl^{-}) of pH 7.8 for positive bias (a) and negative bias (b).

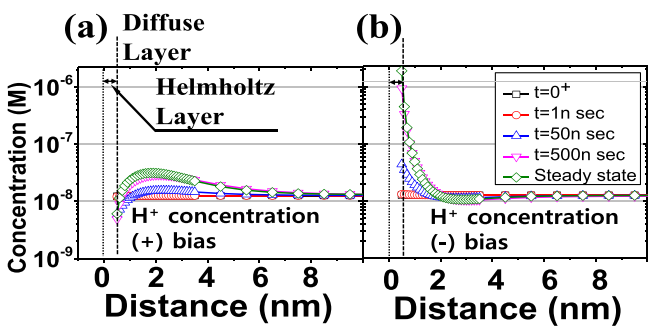

FIG. 2. Calculated H^{+} distribution representing the surface pH with buffer under positive (a) and negative bias (b).

The interaction of the CNT defect ($-COO^-$) with albumin follows the reaction as

$$C - Albumin^{n-} \underset{K_{a6}}{\Longleftrightarrow} Albumin^{n-} + C, \tag{5}$$

where C is COO^- (binding site), $Albumin^{n-}$ is the albumin in the electrolyte solution, and K_{a6} (5.3×10^{-5} M^{-1})[20] is the association constant between CNT surface and albumin. The system detects the albumin adsorption on CNT surface by the difference of the binding number before and after the applying the pulse train to the device.

The suppression of the albumin adsorption on the CNT surface under the application of pulse train is due to the decrease of $Albumin^{n-}$ in Eq. (5). The decrease of albumin concentration at the surface can be understood from the simulation study in terms of the albumin charging state and surface pH as follows. Before the pulse transition (when the bias stays at high or low level), the buffer reaction and potential difference between the CNT channel and liquid set the H^+ concentration to be its steady-state value as described in Figure 2, and the flux of albumin at the surface is negligible because the electric field at the surface is small. However, immediately after the step pulse voltage is applied between the channel and the bulk electrolyte solution, the electric double layer (EDL) is extended making the high electric field between the channel and bulk of electrolyte within τ_{RC}, which can be estimated $\sim O(10^{-6})$ seconds (NaCl 150 mM). At this moment, as schematically shown in Figure 3(a), the H^+ are congregated (A: falling edge) and are swept away (B: rising edge) by high external electric field due to the extended EDL after the pulse bias. The behaviors of the electric field and τ_{RC} can be confirmed by the simulation result, as shown in Figure 3(b).

The point is that the outward flux from the electrode surface at the falling edge is much larger than the inward flux at the rising edge. This is because the charging state of the albumin is different for those two edges. As shown in Figure 2, the application of negative bias changes the surface pH in the buffer solution, and thus, H^+ concentrations for falling and rising edges are different. Hence, from Eq. (4), the net charge of albumin in the vicinity of the electrical channel is changed from more negative to less negative (A: falling edge) and from less negative to more negative (B: rising edge) as shown in Figure 3(b), and thus, the drift terms of albumin in Eq. (1) for both cases are different. As a result, the more negatively charged albumins at falling edge are more swept away (lager outward flux) but the less negatively charged albumins are less congregated at rising edge (smaller inward flux) by high external electric field in the transient state within τ_{RC}. Therefore, the concentration of albumin near the surface decreases as the pulse train is applied, and thus, the albumin adsorption in Eq. (5) is suppressed.

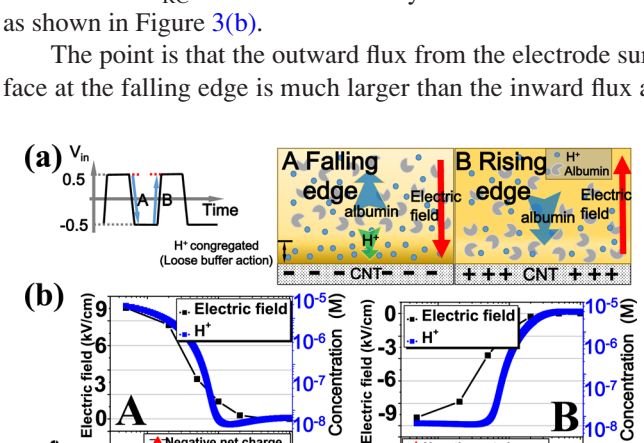

FIG. 3. (a) Schematic diagram of the H^+ and albumin in the vicinity of the electrode in an aqueous solution with respect to falling (A) and rising (B) edge of the applied pulse train. The pH of the solution can be altered locally by the applying voltage. The surface pH can be lower than the bulk pH with negative bias, and it can lead to a less negatively charged albumin. (b) Electric field, H^+ and charging state of albumin profiles in falling edge (A) and rising edge (B) on transient state. The electrode bias voltage is set to 0.5 V → −0.5 V (falling edge) and −0.5 V → 0.5 V (rising edge). $ratio = \frac{Charging\ state\ of\ albumin(at\ surface)}{Charging\ state\ of\ albumin(at\ bulk)}$.

Figure 4 shows the simulation result on the normalized adsorption of albumin *vs.* time during the application of pulse trains. At $t = 0$ s, the pulse train is applied to the electrode in the buffer with the albumin. As shown in the inset of Figure 4, the normalized adsorption of albumin was measured at the rising edges (before changing the bias) of the pulse train, as denoted with arrows. High external electric field at falling or rising edge induces the unbalanced outward and inward flux of the negative charged albumin on transient state, so that the concentration of adsorbed albumin is decreased as the system experiences the pulse transitions. Therefore, the simulation result in Figure 4 clearly indicates that the pulse train can suppress the albumin adsorption at the CNT surface so that the nonspecific binding can be diminished achieving high selectivity of electrical biosensors.

As the experiments signatures to support the theoretical simulations in Figures 3 and 4, we have performed two experiments: (1) an electrical modulation of CNT channel current in serum assuming that the modulation is mainly made by the nonselective adsorption of albumin and (2) an optical experiment with the albumin optically tagged. All chemicals and solvents used in these experiments were of reagent grade, and were used without further purification. Fluorescent conjugated albumin samples were purchased from Bioneer, Inc. (Korea). Human serum samples from

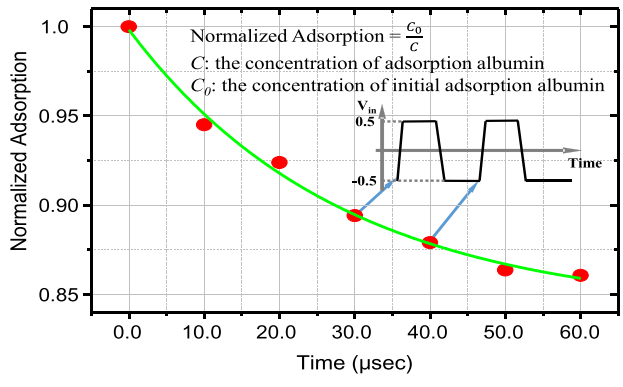

FIG. 4. The effect of the pulse train to albumin adsorption on CNT. Corresponding adsorption ratio with respect to the time during the application of pulse train. Each point is sampled at the rising edges (inset).

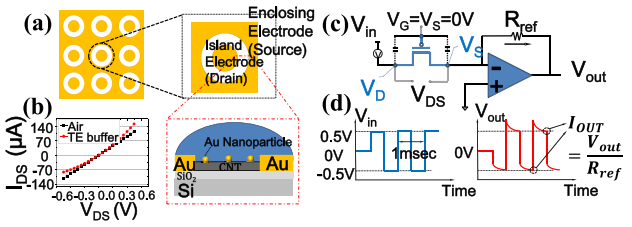

FIG. 5. (a) Conceptual diagram of sensor array, and structure of individual sensor device. Concentric structure consists of drain and source electrode in electrolyte which gives self gating effect. (b) The current versus voltage characteristics of a CNN fabricated on concentric structure with the floated gate. (c) The equivalent circuit diagram of the electrical set up. Configuration for pulse biasing in the sensor device, (d) applied input bias and output.

human male AB plasma (H4522) and PBS (NaCl: 150 mM, pH 7.6) were purchased from Sigma-Aldrich, Inc. (Korea).

In order to test the applicability of the pulse bias scheme in the PoC applications without the washing step to remove the nonselectively bound molecules, the behavior of the CNT current under serum without the probe-target molecules has been studied. The experimental configuration includes a CNT transistor, as depicted in Figure 5. The unique asymmetric feature of the two electrodes system is manifested as the asymmetric *I-V* characteristics acting like a normally turned on pMOSFET as shown in Figure 5(b), known as "self gating effect."[25] The electrical signal of carbon nanotube networks (CNN) on the test pattern was measured using the electrical set up to implement the pulse bias scheme as shown in Figure 5(c). A Tektronix AFG3021 pulse generator was used for the pulsed measurement. The electrical readout signal was measured by a Tektronix DPO7104 digital oscilloscope. The real time measurement under the pulse train during the experiment collects the output voltage in the steady state as shown in Figure 5(d).

Figure 6(a) shows real time characteristics for the DC (0.5 V) and pulse train (±0.5 V, 10 Hz, 1 kHz, 100 kHz) bias on CNN devices after injection of serum. The conductance decrease of the pulse biased device with high frequency (1kHz, 100kHz) is 5%, while that of the DC biased and the pulse biased with low frequency (10Hz) is approximately 40%. The real time measurement results less than 10 Hz are almost the same as the case for DC bias, and more than 1 kHz shows that the CNN surface is not affected by the nonspecific bio molecules in serum.

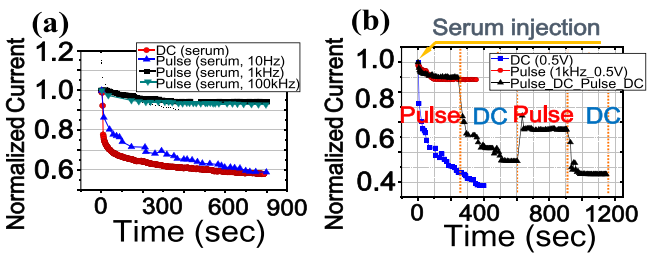

FIG. 6. (a) Real-time conductance change upon adding serum under the DC and pulse train conditions with an amplitude of ±0.5 V and frequency of 10Hz, 1kHz, and 100 kHz. (b) Current *vs.* time for the device with various biasing conditions (Red circles: pulse train with ±0.5 V amplitude and 1 kHz frequency; Blue squares: DC biasing conditions with 0.5 V; Black triangles: consecutive pulse train and DC biasing).

Nonspecifically bound bio molecules on the CNN channel gives an effect to the doping the CNT so that the current is reduced.[26] Also, nonspecifically adsorbed bio molecules between the CNN channel and electrode decrease the transparency of the metal-CNT Schottky barriers,[27] thereby reducing the p-type conduction due to changes in the CNT-metal work function difference. However, in pulse train (more than 1 kHz), the pulse bias induces the interruption of bio molecule adsorption on the CNN surface.

The additional experiments were performed to confirm the effect of the pulse train in serum more clearly. In Figure 6(b), the real-time responses of the devices under the consecutive pulse train, DC bias (pulse train: 1 kHz, 0.5 V, DC: 0.5 V) are shown. In case of applying the pulse train, a slight decrease in conductance was observed after injection of serum, which is consistent with the result in Figure 6(a). Subsequently, applying DC bias, the device showed a rapid decrease in the current. Considering the effect of the pulse train, the adsorption of albumin is surprisingly small for the sample undergoing the pulse train (1 kHz, 0.5 V), compared with the sample undergoing the DC bias.

To directly confirm the effect of the pulse train to the nonspecific binding of bio molecules, a fluorescent conjugated albumin (excitation: 650 nm, emission: 688 nm) in PBS solution was employed. For the adsorption, the CNN device was exposed to a buffer solution with fluorescent labeled albumin for 1200 sec at room temperature. After albumin adsorption under various bias condition (pulse train, DC bias), images were obtained on the metal and in the gap between the electrodes with a confocal laser scanning microscope (Leica Microsystems) using a 20 × lens (NA 0.7) with an excitation wavelength of 633 nm and an emission filter range from 675 to 700 nm. In Figure 7(a), the confocal microscopic image of the device that undergone the pulse bias during binding with the albumin is shown. Compared with the control device (Figure 7(b)) without the binding experiment, there is no appreciable difference in the fluorescence intensity implying that the pulse train suppresses the nonspecific binding. However, the device that undergone the DC bias (Figure 7(c)) shows a significant increase in the fluorescence intensity.

From those two experiments in Figures 6 and 7, it is clearly confirmed that the pulse train can indeed suppress the adsorption of albumin on the CNT. And, the trend from the

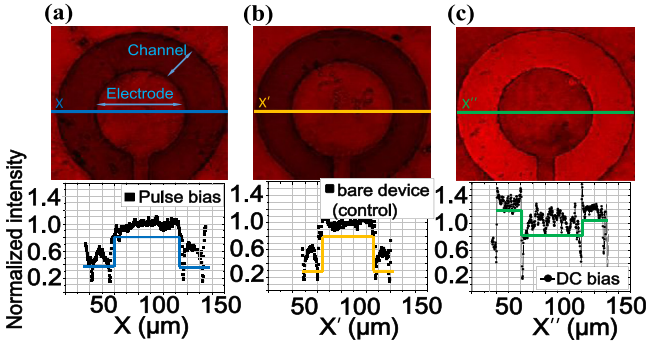

FIG. 7. Confocal microscopic image of the devices after nonspecific binding with the fluorescent conjugated albumin; (a) device under the pulse bias (1 kHz, ±0.5 V), (b) the control device without the albumin adsorption experiment, and (c) device under DC bias (0.5 V).

experiments is similar to that predicted by the simulation shown in Figure 4. Although the simulation device structure does not directly match with the experimental one, the agreement in the trend implies the justification of the pulse train method to suppress the adsorption of albumin on CNT surface. It would be tremendous amount work of its own value to develop the simulator considering the three dimensional structure and all the proteins contained in serum. The purpose of the simulation in this work is to understand the major physical mechanisms responsible for the experimental finding—suppression of the albumin on the CNT surface under the electrical pulse bias condition.

We have presented a numerical simulation for the nonspecific binding of biomolecules in serum to the pulse train. From the simulation, we showed that the charging state of albumin during the falling edge is different from that of the rising edge of the pulse train resulting the suppression of albumin at the surface and thus the nonspecific adsorption of albumin is suppressed. In addition, both the electrical modulation of the CNT's and optical measurements under the electrical pulse train suppress the adsorption of charged molecules in serum. The effect may be called the "electrical passivation of nonspecific binding" in the electrical biosensor. Further work on this general principle can be extended to sensing the hybridization event for other charged molecules such as proteins.

This research was supported by the Pioneer Research Center Program through the National Research Foundation of Korea funded by the Ministry of Science, ICT & Future Planning (NRF-2012-0009555) and by the Center for Integrated Smart Sensors (CISS-2012054186) funded by the Ministry of Science of Korea.

[1]J. Homola, S. S. Yee, and G. Gauglitz, Sens. Actuators B **54**(1), 3–15 (1999).
[2]P. K. Jain and M. A. El-Sayed, J. Phys. Chem. C **111**(47), 17451–17454 (2007).
[3]M. Caldow, S. L. Stead, J. Day, M. Sharman, C. Situ, and C. Elliott, J. Agric. Food Chem. **53**(19), 7367–7370 (2005).
[4]E. Souteyrand, J. P. Cloarec, J. R. Martin, C. Wilson, I. Lawrence, S. Mikkelsen, and M. F. Lawrence, J. Phys. Chem. B **101**(15), 2980–2985 (1997).
[5]H. Berney, J. West, E. Haefele, J. Alderman, W. Lane, and J. Collins, Sens. Actuators B **68**(1), 100–108 (2000).
[6]J. S. Daniels and N. Pourmand, Electroanalysis **19**(12), 1239–1257 (2007).
[7]Y. Cui, Q. Wei, H. Park, and C. M. Lieber, Science **293**(5533), 1289–1292 (2001).
[8]M. Pacios, I. Martin-Fernandez, X. Borrise, M. del Valle, J. Bartroli, E. Lora-Tamayo, P. Godignon, F. Perez-Murano, and M. J. Esplandiu, Nanoscale **4**(19), 5917–5923 (2012).
[9]J. Kleijn and W. Norde, Heterog. Chem. Rev. **2**, 157–172 (1995).
[10]O. Moradi, M. S. Maleki, and S. Tahmasebi, Fullerenes, Nanotubes Carbon Nanostruct. **21**(8), 733–748 (2013).
[11]J. Shi, J. Guo, G. Bai, C. Chan, X. Liu, W. Ye, J. Hao, S. Chen, and M. Yang, Biosens. Bioelectron. **65**, 238–244 (2015).
[12]Y. X. Huang, X. C. Dong, Y. X. Liu, L. J. Li, and P. Chen, J. Mater. Chem. **21**(33), 12358–12362 (2011).
[13]J. M. Woo, S. H. Kim, H. Chun, S. J. Kim, J. Ahn, and Y. J. Park, Lab Chip **13**(18), 3755–3763 (2013).
[14]D. R. Lide, *CRC Handbook of Chemistry and Physics* (CRC Press, 2004).
[15]N. Meechai, A. M. Jamieson, and J. Blackwell, J. Colloid Interface Science **218**(1), 167–175 (1999).
[16]H. J. Kwon, Ph.D. thesis, Seoul National University, 2012.
[17]J. Chen, M. J. Dyer, and M.-F. Yu, J. Am. Chem. Soc. **123**(25), 6201–6202 (2001).
[18]M. W. Marshall, S. Popa-Nita, and J. G. Shapter, Carbon **44**(7), 1137–1141 (2006).
[19]M. A. Brusatori, Y. Tie, and P. R. Van Tassel, Langmuir **19**(12), 5089–5097 (2003).
[20]A. Javadi, S. Mirdamadi, M. Faghihisani, S. Shakhesi, and R. Soltani, Fullerenes, Nanotubes Carbon Nanostruct. **21**(5), 436–447 (2013).
[21]J.-M. Woo, S. H. Kim, and Y. J. Park, in *Proceedings of the 17th International Conference on Simulation of Semiconductor Processes and Devices (SISPAD)* (IEEE, 2012), pp. 177–180.
[22]J.-M. Woo, S. H. Kim, and Y. J. Park, in the Proceedings of the 8th International Workshop on Compact Modeling (IWCM), 2011.
[23]F. M. Richards, J. Mol. Biol. **82**(1), 1–14 (1974).
[24]H. P. Erickson, Biol. Proced. Online **11**(1), 32–51 (2009).
[25]D. W. Kim, G. S. Choe, S. M. Seo, J. H. Cheon, H. Kim, J. W. Ko, I. Y. Chung, and Y. J. Park, Appl. Phys. Lett. **93**(24), 243115 (2008).
[26]A. B. Artyukhin, M. Stadermann, R. W. Friddle, P. Stroeve, O. Bakajin, and A. Noy, Nano Lett. **6**(9), 2080–2085 (2006).
[27]S. Heinze, J. Tersoff, R. Martel, V. Derycke, J. Appenzeller, and P. Avouris, Phys. Rev. Lett. **89**(10), 106801 (2002).